5184 *Macromolecules* **2010**, *43*, 5184–5187
DOI: 10.1021/ma100813m

Macromolecules
COMMUNICATION TO THE EDITOR

Unique Thermo-Induced Sequential Gel−Sol−Gel Transition of Responsive Multiblock Copolymer-Based Hydrogels

Jinming Hu, Zhishen Ge,* Yueming Zhou, Yanfeng Zhang, and Shiyong Liu*

CAS Key Laboratory of Soft Matter Chemistry, Department of Polymer Science and Engineering, Hefei National Laboratory for Physical Sciences at the Microscale, University of Science and Technology of China, Hefei, Anhui 230026, China

Received April 14, 2010
Revised Manuscript Received May 21, 2010

Responsive polymeric hydrogels that can reversibly switch between free-flowing liquid and free-standing gel states have aroused tremendous interest in the past few decades due to their applications in controlled drug delivery, tissue engineering, and sensors.[1] Gelation and the reverse process can be facilely triggered by external stimuli such as pH, temperature, ionic strength, biomolecules, light, and magnetic field or a proper combination of them.[1b,2] Previously, a variety of thermosensitive hydrogels as injectable materials have been fabricated from amphiphilic and double hydrophilic diblock or triblock copolymers at relatively high critical gelation concentrations (CGC, >15−20 wt %) via the micelle packing mechanism.[1h,2c,3] They mainly exhibit three types of thermo-induced phase switching behavior including gel−sol, sol−gel, and sol−gel−sol transitions depending on the sequence arrangement and relative chain lengths of hydrophilic and hydrophobic blocks. On the other hand, amphiphilic multiblock copolymers of $(AB)_n$ type demonstrate enhanced gelation capability with lower CGCs and improved rheological properties via the interconnected micelle-network mechanism due to their unique chain architectures.[4]

It is worth noting that previous examples of thermosensitive polymeric hydrogels mainly exploit hydrophobic interactions as the driving force to induce physical gelation.[5] Concerning thermosensitive double hydrophilic block copolymers (DHBCs), a few examples have been reported by Laschewsky et al.[6] and Armes et al.,[7] in which the two blocks possess lower and upper critical solution temperature (LCST and UCST) phase behaviors, respectively. Thus, they exhibit thermo-induced micelle−unimer−micelle transitions in aqueous solution. As for block copolymer hydrogels, the counterpart phenomenon, thermo-induced sequential gel−sol−gel transition with relatively low CGC values, has not been experimentally achieved yet. Hydrogels possessing this novel property exist in the free-flowing "soft" state only within a specific temperature range, and apart from this, gelation occurs to produce a "hard" semisolid material. This might be quite helpful if they are being considered as candidates for smart valves and recyclable carriers.

The current work is based on the idea of thermo-regulating the relative dominance of two types of supramolecular interactions, namely hydrophobic and electrostatic interactions in aqueous solutions of responsive multiblock copolymers (Scheme 1). pH-responsive poly(4-vinylpyridine) (P4VP) and thermosensitive random copolymer of *N*-isopropylacrylamide (NIPAM) and *N*, *N*-dimethylacrylamide (DMA), P(NIPAM-*co*-DMA), were chosen as the two chain sequences alternately arranged in *m*-P(NIPAM-*co*-DMA)-*b*-P4VP multiblock copolymers. It has been previously established that protonated polymers such as P4VP in dilute aqueous solution can exhibit a UCST-type phase behavior in the presence of multivalent inorganic or organic counterions.[8] Thus, strong electrostatic interactions between protonated P4VP sequences in *m*-P(NIPAM-*co*-DMA)-*b*-P4VP and the counterion cross-linker, sodium 2,6-naphthalene disulfonate (NDSNa), exist at low temperatures and result in gelation, whereas at elevated temperatures, electrostatic interactions tend to be disintegrated and a gel−sol transition can be obtained. PNIPAM has been well-recognized as a thermosensitive polymer with a LCST of ∼32 °C.[9] Thermogelling of PNIPAM-containing triblock copolymers has been previously reported by McCormick et al.[10] and Armes et al.[11] P(NIPAM-*co*-DMA) block was chosen as another type of polymer sequence in *m*-P(NIPAM-*co*-DMA)-*b*-P4VP multiblock to elevate its LCST compared to PNIPAM homopolymers, aiming at clear observation of the unique thermo-induced sequential gel−sol−gel phase transition behavior.

Synthetic routes employed for the preparation of *m*-P(NIPAM-*co*-DMA)-*b*-P4VP multiblock copolymers are shown in Scheme 1a. *m*-P(NIPAM-*co*-DMA) precursor was obtained via reversible addition−fragmentation chain transfer (RAFT) polymerization of NIPAM and DMA monomers by using polytrithiocarbonate (PTTCA) with a degree of polymerization (DP) of ∼20 as the macroRAFT agent.[12] *m*-P(NIPAM-*co*-DMA)-*b*-P4VP multiblock copolymers were then prepared via RAFT polymerization of 4VP monomer using *m*-P(NIPAM-*co*-DMA) as macroRAFT agent in the presence of a redox initiator system.[13] DPs of P(NIPAM-*co*-DMA) and P4VP sequences of multiblock copolymers were estimated from ^{1}H NMR analysis (see the Supporting Information, Figure S1). Two multiblock copolymers with varying DPs of P4VP sequences, *m*-P(NIPAM$_{0.51}$-*co*-DMA$_{0.49}$)$_{138}$-*b*-P4VP$_{87}$ and *m*-P(NIPAM$_{0.51}$-*co*-DMA$_{0.49}$)$_{138}$-*b*-P4VP$_{136}$, were thus obtained.

The block numbers (p) of the precursor, *m*-P(NIPAM-*co*-DMA)$_m$, and multiblock copolymers, *m*-P(NIPAM-*co*-DMA)$_m$-*b*-P4VP$_n$, were estimated by cleaving them into individual P(NIPAM-*co*-DMA)$_m$ and P4VP$_{n/2}$-*b*-P(NIPAM-*co*-DMA)$_m$-*b*-P4VP$_{n/2}$ chains, respectively, in the presence of excess 2,2-azobis(isobutyronitrile) (AIBN).[12,14] The cleaved products are relatively monodisperse (M_w/M_n < 1.2), indicating that RAFT polymerization processes were conducted in a relatively controlled manner (see the Supporting Information, Figure S2). From GPC analysis, the block numbers (p) of the precursor and two multiblock copolymers, *m*-P(NIPAM$_{0.51}$-*co*-DMA$_{0.49}$)$_{138}$-*b*-P4VP$_{87}$ and *m*-P(NIPAM$_{0.51}$-*co*-DMA$_{0.49}$)$_{138}$-*b*-P4VP$_{136}$, were determined to be 5.7, 3.8, and 3.5, respectively.

Within *m*-P(NIPAM-*co*-DMA)-*b*-P4VP multiblock copolymers, P(NIPAM-*co*-DMA) and protonated P4VP sequences are expected to exhibit LCST and UCST type of phase behaviors, respectively, in the presence of NDSNa. In dilute aqueous solutions, the aggregation behavior of *m*-P(NIPAM$_{0.51}$-*co*-DMA$_{0.49}$)$_{138}$-*b*-P4VP$_{87}$ has been investigated at first by ^{1}H NMR analysis at pH 1.5 in the presence of NDSNa ([4VPH$^+$]/[SO$_3^-$] = 1/1) (Figure S3). At 40 °C, NMR resonance signals corresponding to P(NIPAM-*co*-DMA) and P4VP sequences are visible, and the peak integral ratio characteristic of both chain sequences agrees quite well with that obtained by NMR analysis in $CDCl_3$, suggesting that the multiblock dissolves as unimers

*To whom correspondence should be addressed. E-mail: gezs@mail.ustc.edu.cn (Z.G.), sliu@ustc.edu.cn (S.L.).

 Published on Web 05/25/2010

Scheme 1. (a) Synthetic Routes Employed for the Preparation of Multiblock Copolymers Comprising Thermoresponsive and pH-Responsive Sequences Arranged in an Alternate Manner, *m*-P(NIPAM-*co*-DMA)-*b*-P4VP, via Successive Reversible Addition−Fragmentation Chain Transfer (RAFT) Polymerizations; (b) Schematic Representation for Thermo-Induced Sequential Gel−Sol−Gel Transitions of *m*-P(NIPAM-*co*-DMA)-*b*-P4VP Multiblock Hydrogels in the Presence of 1.0 equiv of Sodium 2,6-Naphthalenedisulfonate (NDSNa) at pH 1.5

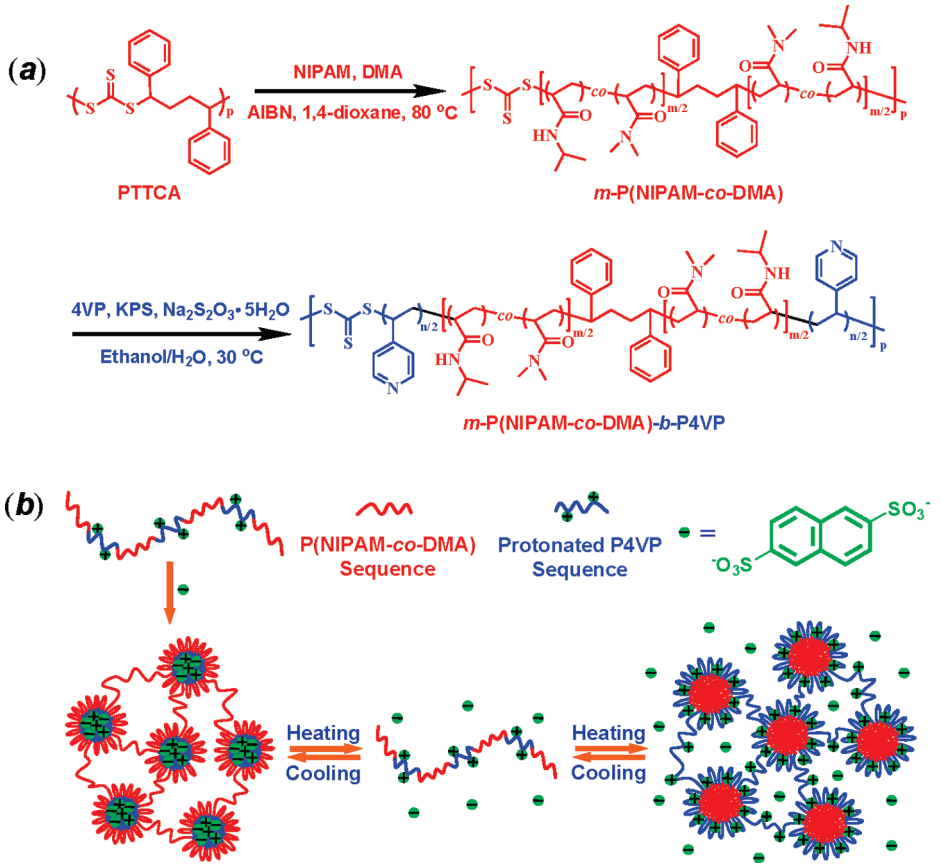

(Figure S3). However, at 5 °C, intensity of resonance signals characteristic of protonated P4VP sequence (*e* and *f*) dramatically weakens, suggesting the formation of aggregates with protonated P4VP/NDSNa complex as the core and well-solvated P(NIPAM-*co*-DMA) sequences as the corona. Upon heating to 55 °C, characteristic signals of P(NIPAM-*co*-DMA) at δ = 3.0 and 3.9 ppm (*b* and *c*) exhibit a clear decrease in intensity, accompanied by the restoration of peaks *e* and *f* characteristic of protonated P4VP. This suggests the formation of another type of aggregates with inverted nanostructures at elevated temperatures, as compared to that at 5 °C.

Dynamic light scattering (DLS) was further employed to characterize the thermo-induced inverting of self-assembled aggregates in the aqueous solution of *m*-P(NIPAM$_{0.51}$-*co*-DMA$_{0.49}$)$_{138}$-*b*-P4VP$_{87}$ (0.3 g/L, pH 1.5, [4VPH$^+$]/[SO$_3^-$] = 1/1; Figure 1a; Table S1). In the temperature range of 5−30 °C, aggregates with P4VP/DNSNa complex cores are relatively stable with an average hydrodynamic radius, $\langle R_h \rangle$, of ~40 nm, though we can discern a slight decrease of scattering intensity. Above 30 °C, micelles start to dissociate due to the weakening of ionic complexation between protonated P4VP and NDSNa, which is accompanied by the sharp decrease of both $\langle R_h \rangle$ and scattering intensity. In the temperature range of 37−46 °C, scattering intensity exhibits a local plateau with $\langle R_h \rangle$ being ~8−10 nm, indicating the existence of unimer state. Above 46 °C, the dramatic increase of $\langle R_h \rangle$ and scattering intensity can be clearly ascribed to the collapse of P(NIPAM-*co*-DMA) sequences due to its LCST phase behavior and the formation of P(NIPAM-*co*-DMA)-core aggregates with $\langle R_h \rangle$ being ~186 nm at 56 °C. Temperature-dependent optical transmittance measurements have further confirmed the above conclusion (Figure S4). In the temperature range of 35−47 °C, the aqueous mixture of *m*-P(NIPAM$_{0.51}$-*co*-DMA$_{0.49}$)$_{138}$-*b*-P4VP$_{87}$ and NDSNa (5.0 g/L, pH 1.5, [4VPH$^+$]/[SO$_3^-$] = 1/1) is clear. Apart from this temperature range, stable dispersions with bluish tinge, which is characteristic of colloidal aggregates, are obtained. This suggests the formation of two types of aggregates with inverted core−shell nanostructures.

We are quite curious about the thermo-induced switching between gel and sol states for aqueous solutions of P(NIPAM-*co*-DMA)$_m$-*b*-P4VP$_n$ multiblock copolymers at high concentrations. Previous reports revealed that multiblock copolymers exhibit stronger gelation capability compared to those of diblock and triblock copolymers in terms of CGCs and gel storage modulus due to unique chain topologies of the former.[4] The alternate arrangement of chain sequences in multiblock copolymers favors gelation via the interconnected micelle network mechanism. As shown in Figure 1c, we can observe gel, sol, and gel states at 5, 35, and 55 °C, respectively, for the aqueous solution of *m*-P(NIPAM$_{0.51}$-*co*-DMA$_{0.49}$)$_{138}$-*b*-P4VP$_{87}$ multiblock copolymer at 10 wt % (pH 1.5, [4VPH$^+$]/[SO$_3^-$] = 1/1). To the best of our knowledge, this represents the first example of thermo-induced sequential gel−sol−gel transition for block copolymer-based physical hydrogels (Scheme 1b).

A comparison to the aggregation properties of the multiblock in dilute aqueous solution (Figure 1a, Figures S3 and S4) reveals that at 5 °C ionic complexation between protonated P4VP and NDSNa is responsible for the physical gelation, which leads to insolubility of P4VP sequences. Moreover, soluble P(NIPAM-*co*-DMA) sequences can stabilize the aggregates at low concentrations and bridge them at high concentrations to form macroscopic physical hydrogels. Scheme 1b illustrates the possible chain packing model within hydrogels formed at low temperatures.

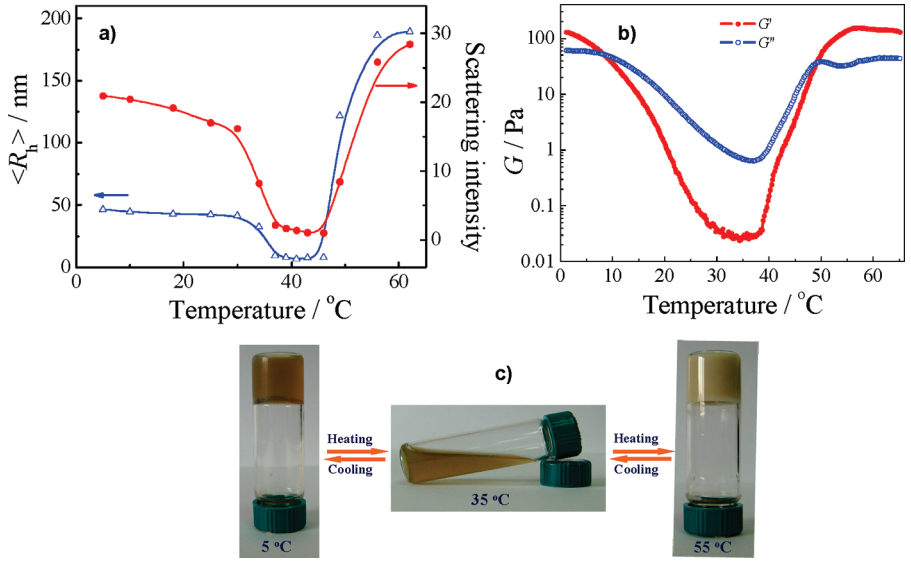

Figure 1. (a) Temperature dependence of average hydrodynamic radius, $\langle R_h \rangle$, and light scattering intensity obtained for the aqueous solution (pH 1.5, 0.3 g/L) of *m*-P(NIPAM$_{0.51}$-*co*-DMA$_{0.49}$)$_{138}$-*b*-P4VP$_{87}$ in the presence of NDSNa ([4VPH$^+$]/[SO$_3^-$] = 1/1). (b) Temperature dependence of storage modulus G' and loss modulus G'' obtained for 10 wt % aqueous solution (pH 1.5) of *m*-P(NIPAM$_{0.51}$-*co*-DMA$_{0.49}$)$_{138}$-*b*-P4VP$_{87}$ in the presence of NDSNa ([4VPH$^+$]/[SO$_3^-$] = 1/1). The shear strain γ was 1.0%, and angular frequency ω is 1.0 rad/s. (c) digital photographs recorded for 10 wt % aqueous solution (pH 1.5) of *m*-P(NIPAM$_{0.51}$-*co*-DMA$_{0.49}$)$_{138}$-*b*-P4VP$_{87}$ at 5 °C (gel), 35 °C (sol), and 55 °C (gel) in the presence of NDSNa ([4VPH$^+$]/[SO$_3^-$] = 1/1).

Upon heating to intermediate temperatures (35 °C), ionic complexation between protonated P4VP and NDSNa is greatly weakened, and both P(NIPAM-*co*-DMA) and protonated P4VP sequences are soluble, resulting in the sol state. Further heating above the LCST of P(NIPAM-*co*-DMA) sequences leads to the formation of another type of physical hydrogels due to hydrophobic interactions. It is worthy of noting that the two types of hydrogels formed at low and high temperatures possess intriguing "inverted" microstructures in terms of the aggregated core and bridging chain segments (Scheme 1b). Thus, we successfully achieved a proof-of-concept example of thermo-induced sequential gel−sol−gel transition from responsive multiblock copolymers by thermo-tuning the relative dominance of two types of noncovalent interactions, namely, electrostatic and hydrophobic interactions. It should be noted that the thermo-induced gel−sol−gel transitions are completely reversible, i.e., cooling from the gel state at 55 °C to 5 °C can realize sequential gel−sol−gel transition in the reverse order, as compared to that observed in the heating process. This reflects the dynamic nature of typical physical hydrogels.[1−3,15]

The storage modulus G' and loss modulus G'' can reveal the energy stored and dissipated upon hydrogel deformation. The higher storage modulus relative to the loss modulus ($G' > G''$) has been recognized as one of the characteristics to differentiate between gel and sol states.[15] Rheological measurements were then conducted for 10 wt % aqueous solutions of *m*-P(NIPAM-*co*-DMA)$_m$-*b*-P4VP$_n$ multiblock copolymers (pH 1.5, [4VPH$^+$]/[SO$_3^-$] = 1/1), and the results are shown in Figure 1c. In the temperature range of 8−49 °C, G' is lower than G'', which is typical of Newtonian fluid. In contrast, below 8 °C or above 49 °C, G' is greater than G'' in both cases, which is characteristic of an elastic gel. Thus, during the sequential heating process, the critical gel−sol and sol−gel transition temperatures are determined to be 8 and 49 °C, respectively, by rheology measurements. Moreover, both G' and G'' exhibit a local minimum in the intermediate temperature range, which reasonably agrees with the aggregation behavior obtained at low concentrations (Figure 1, Figures S3 and S4). The critical gel−sol−gel transition temperatures can be further tuned by relative block lengths of P(NIPAM-*co*-DMA) and P4VP sequences. Rheology measurements revealed

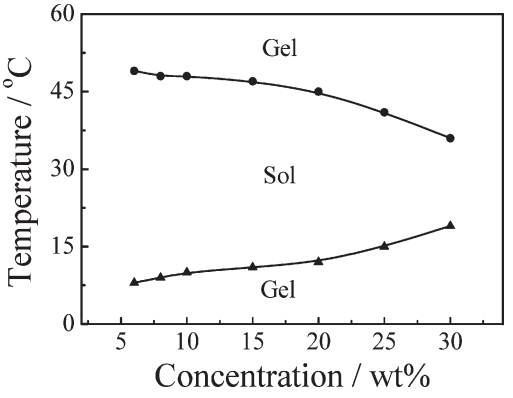

Figure 2. Phase diagrams obtained for the aqueous dispersion (pH 1.5) of *m*-P(NIPAM$_{0.51}$-*co*-DMA$_{0.49}$)$_{138}$-*b*-P4VP$_{87}$ multiblock copolymer at varying polymer concentrations in the presence of NDSNa ([4VPH$^+$]/[SO$_3^-$] = 1/1).

that the aqueous solution of *m*-P(NIPAM$_{0.51}$-*co*-DMA$_{0.49}$)$_{138}$-*b*-P4VP$_{136}$ (10 wt %, pH 1.5, [4VPH$^+$]/[SO$_3^-$] = 1/1) exhibits critical gel−sol and sol−gel temperatures of 14 and 51 °C, respectively (Table S1).

The phase diagram of *m*-P(NIPAM$_{0.51}$-*co*-DMA$_{0.49}$)$_{138}$-*b*-P4VP$_{87}$ multiblock copolymer in aqueous solution (pH 1.5) in the presence of NDSNa ([4VPH$^+$]/[SO$_3^-$] = 1/1) is shown in Figure 2, and critical transition temperatures were determined via the tube inverting approach during the heating process. In the polymer concentration range of 6−30 wt %, the phase diagram comprises of three regions (gel, sol, and gel) divided by the gel−sol and sol−gel transition boundaries. We can tell from Figure 2 that gel−sol transition temperatures slightly increase with polymer concentrations, which is contrary to the concentration dependence of sol−gel transitions occurred at elevated temperatures. At polymer concentrations below 6 wt %, we cannot observe the sequential gel−sol−gel transition and gel state in the lower temperature region can not be obtained. It is interesting to note that P4VP$_{44}$-*b*-P(NIPAM-*co*-DMA)$_{69}$-*b*-P4VP$_{44}$ triblock copolymers cleaved from the corresponding multiblocks (Figure S2) also exhibit gel−sol−gel transition behavior in the presence of

equimolar NDSNa upon sequential heating, provided that the triblock polymer concentrations are higher than ~20 wt %.[1d,2c,10,11,16] In the current case, the multiblock architecture of *m*-P(NIPAM$_{0.51}$-*co*-DMA$_{0.49}$)$_{138}$-*b*-P4VP$_{87}$ renders it possible to observe the thermo-induced sequential gel−sol−gel transition at polymer concentrations as low as 6 wt %.

In summary, responsive *m*-P(NIPAM-*co*-DMA)-*b*-P4VP multiblock copolymers were synthesized via consecutive RAFT polymerizations using polytrithiocarbonate as the mediating agent. In dilute aqueous solution (pH 1.5), the mixture of *m*-P(NIPAM$_{0.51}$-*co*-DMA$_{0.49}$)$_{138}$-*b*-P4VP$_{87}$ and NDSNa ([4VPH$^+$]/[SO_3^-] = 1/1) can form two types of aggregates with inverted nanostructures at low and high temperature ranges, respectively. At polymer concentrations higher than 6 wt %, the equimolar multiblock/NDSNa mixture exhibit unique thermo-induced sequential gel−sol−gel transition behavior by thermo-regulating the relative dominance of two types of supramolecular interactions, namely hydrophobic and electrostatic interactions. Moreover, the critical gel−sol−gel transition temperatures can be facilely tuned by adjusting relative sequence lengths and polymer concentrations. Intriguing properties of this novel type of responsive multiblock copolymer-based hydrogels at concentrations as low as 6 wt % augur well for their potential applications as smart materials in drug delivery, sensors, valves, and actuators. Further work toward this aspect is currently underway.

Acknowledgment. The financial support of National Natural Scientific Foundation of China (NNSFC) Project (20874092) and Specialized Research Fund for the Doctoral Program of Higher Education (SRFDP) is gratefully acknowledged.

Supporting Information Available: Experimental details and spectroscopic/analytical data of ^{1}H NMR, GPC, and UV−vis transmittance. This material is available free of charge via the Internet at http://pubs.acs.org.

References and Notes

(1) (a) Kopecek, J. *Biomaterials* **2007**, *28*, 5185–5192. (b) He, C. L.; Kim, S. W.; Lee, D. S. *J. Controlled Release* **2008**, *127*, 189–207. (c) Peppas, N. A.; Hilt, J. Z.; Khademhosseini, A.; Langer, R. *Adv. Mater.* **2006**, *18*, 1345–1360. (d) Lee, K. Y.; Mooney, D. J. *Chem. Rev.* **2001**, *101*, 1869–1879. (e) Bromberg, L. E.; Ron, E. S. *Adv. Drug Delivery Rev.* **1998**, *31*, 197–221. (f) Hoffman, A. S. *Adv. Drug Delivery Rev.* **2002**, *54*, 3–12. (g) Qiu, Y.; Park, K. *Adv. Drug Delivery Rev.* **2001**, *53*, 321–339. (h) Yu, L.; Ding, J. D. *Chem. Soc. Rev.* **2008**, *37*, 1473–1481. (i) Hatefi, A.; Amsden, B. *J. Controlled Release* **2002**, *80*, 9–28.

(2) (a) Gil, E. S.; Hudson, S. A. *Prog. Polym. Sci.* **2004**, *29*, 1173–1222. (b) Miyata, T.; Uragami, T.; Nakamae, K. *Adv. Drug Delivery Rev.* **2002**, *54*, 79–98. (c) Jeong, B.; Kim, S. W.; Bae, Y. H. *Adv. Drug Delivery Rev.* **2002**, *54*, 37–51. (d) Schmaljohann, D. *Adv. Drug Delivery Rev.* **2006**, *58*, 1655–1670. (e) Soppimath, K. S.; Aminabhavi, T. M.; Dave, A. M.; Kumbar, S. G.; Rudzinski, W. E. *Drug Dev. Ind. Pharm.* **2002**, *28*, 957–974. (f) Nagarsekar, A.; Crissman, J.; Crissman, M.; Ferrari, F.; Cappello, J.; Ghandehari, H. *Biomacromolecules* **2003**, *4*, 602–607. (g) Stayton, P. S.; Shimoboji, T.; Long, C.; Chilkoti, A.; Chen, G. H.; Harris, J. M.; Hoffman, A. S. *Nature* **1995**, *378*, 472–474. (h) Zheng, P. J.; Hu, X.; Zhao, X. Y.; Li, L.; Tam, K. C.; Gan, L. H. *Macromol. Rapid Commun.* **2004**, *25*, 678–682. (i) Ogoshi, T.; Takashima, Y.; Yamaguchi, H.; Harada, A. *J. Am. Chem. Soc.* **2007**, *129*, 4878–4879. (j) Willet, N.; Gohy, J. F.; Lei, L. C.; Heinrich, M.; Auvray, L.; Varshney, S.; Jerome, R.; Leyh, B. *Angew. Chem., Int. Ed.* **2007**, *46*, 7988–7992. (k) Reinicke, S.; Schmelz, J.; Lapp, A.; Karg, M.; Hellweg, T.; Schmalz, H. *Soft Matter* **2009**, *5*, 2648–2657.

(3) (a) Jeong, B.; Bae, Y. H.; Lee, D. S.; Kim, S. W. *Nature* **1997**, *388*, 860–862. (b) Yu, L.; Zhang, H.; Ding, J. D. *Angew. Chem., Int. Ed.* **2006**, *45*, 2232–2235. (c) Gong, C. Y.; Shi, S. A.; Dong, P. W.; Kan, B.; Gou, M. L.; Wang, X. H.; Li, X. Y.; Luo, F.; Zhao, X.; Wei, Y. Q.; Qian, Z. Y. *Int. J. Pharm.* **2009**, *365*, 89–99. (d) Ruel-Gariepy, E.; Leroux, J. C. *Eur. J. Pharm. Biopharm.* **2004**, *58*, 409–426. (e) Hwang, M. J.; Suh, J. M.; Bae, Y. H.; Kim, S. W.; Jeong, B. *Biomacromolecules* **2005**, *6*, 885–890. (f) Chitkara, D.; Shikanov, A.; Kumar, N.; Domb, A. *J. Macromol. Biosci.* **2006**, *6*, 977–990. (g) Tang, Y.; Singh, J. *Int. J. Pharm.* **2009**, *365*, 34–43.

(4) (a) Wang, X. L.; Mou, Y. R.; Chen, S. C.; Shi, J.; Wang, Y. Z. *Eur. Polym. J.* **2009**, *45*, 1190–1197. (b) Sun, K. H.; Sohn, Y. S.; Jeong, B. *Biomacromolecules* **2006**, *7*, 2871–2877. (c) Loh, X. J.; Goh, S. H.; Li, J. *Biomacromolecules* **2007**, *8*, 585–593. (d) Li, S. M.; Dobrzynski, P.; Kasperczyk, J.; Bero, M.; Braud, C.; Vert, M. *Biomacromolecules* **2005**, *6*, 489–497.

(5) McCormick, C. L.; Sumerlin, B. S.; Lokitz, B. S.; Stempka, J. E. *Soft Matter* **2008**, *4*, 1760–1773.

(6) (a) Virtanen, J.; Arotcarena, M.; Heise, B.; Ishaya, S.; Laschewsky, A.; Tenhu, H. *Langmuir* **2002**, *18*, 5360–5365. (b) Arotcarena, M.; Heise, B.; Ishaya, S.; Laschewsky, A. *J. Am. Chem. Soc.* **2002**, *124*, 3787–3793.

(7) (a) Weaver, J. V. M.; Armes, S. P.; Butun, V. *Chem. Commun.* **2002**, 2122–2123. (b) Cai, Y. L.; Armes, S. P. *Macromolecules* **2004**, *37*, 7116–7122.

(8) (a) Jia, X.; Chen, D. Y.; Jiang, M. *Chem. Commun.* **2006**, 1736–1738. (b) Ma, R. J.; Wang, B. L.; Liu, X. J.; An, Y. L.; Li, Y.; He, Z. P.; Shi, L. Q. *Langmuir* **2007**, *23*, 7498–7504. (c) Wu, K.; Shi, L. Q.; Zhang, W. Q.; An, Y. L.; Zhang, X.; Li, Z. Y.; Zhu, X. X. *Langmuir* **2006**, *22*, 1474–1477. (d) Plamper, F. A.; Schmalz, A.; Ballauff, M.; Muller, A. H. E. *J. Am. Chem. Soc.* **2007**, *129*, 14538–14539.

(9) Schild, H. G. *Prog. Polym. Sci.* **1992**, *17*, 163–249.

(10) (a) McCormick, C. L.; Sumerlin, B. S.; Lokitz, B. S.; Stempka, J. E. *Soft Matter* **2008**, *4*, 1760–1773. (b) Kirkland, S. E.; Hensarling, R. M.; McConaughy, S. D.; Guo, Y.; Jarrett, W. L.; McCormick, C. L. *Biomacromolecules* **2008**, *9*, 481–486.

(11) (a) Li, C. M.; Madsen, J.; Armes, S. P.; Lewis, A. L. *Angew. Chem., Int. Ed.* **2006**, *45*, 3510–3513. (b) Li, C. M.; Tang, Y. Q.; Armes, S. P.; Morris, C. J.; Rose, S. F.; Lloyd, A. W.; Lewis, A. L. *Biomacromolecules* **2005**, *6*, 994–999. (c) Castelletto, V.; Hamley, I. W.; Ma, Y. H.; Bories-Azeau, X.; Armes, S. P.; Lewis, A. L. *Langmuir* **2004**, *20*, 4306–4309.

(12) Zhou, Y. M.; Jiang, K. Q.; Song, Q. L.; Liu, S. Y. *Langmuir* **2007**, *23*, 13076–13084.

(13) Bai, W.; Zhang, L.; Bai, R.; Zhang, G. Z. *Macromol. Rapid Commun.* **2008**, *29*, 562–566.

(14) Perrier, S.; Takolpuckdee, P.; Mars, C. A. *Macromolecules* **2005**, *38*, 2033–2036.

(15) (a) Li, L.; Liu, E. J.; Lim, C. H. *J. Phys. Chem. B* **2007**, *111*, 6410–6416. (b) Sarvestani, A. S.; He, X. Z.; Jabbari, E. *Biomacromolecules* **2007**, *8*, 406–415. (c) Zhang, H.; Yu, L.; Ding, J. D. *Macromolecules* **2008**, *41*, 6493–6499. (d) Choi, Y. Y.; Joo, M. K.; Sohn, Y. S.; Jeong, B. *Soft Matter* **2008**, *4*, 2383–2387.

(16) (a) Mortensen, K.; Batsberg, W.; Hvidt, S. *Macromolecules* **2008**, *41*, 1720–1727. (b) Ma, Y. H.; Tang, Y. Q.; Billingham, N. C.; Armes, S. P.; Lewis, A. L. *Biomacromolecules* **2003**, *4*, 864–868.